

HEAT CONDUCTION IN A LAYERED STRUCTURE WITH AN INTERFACE CRACK USING THE DUAL PHASE LAG MODEL

Zengtao Chen

Department of Mechanical Engineering
 University of Alberta
 Edmonton, AB, Canada
 Zengtao.chen@ualberta.ca

Keqiang Hu

Department of Chemical and Materials Engineering
 University of Alberta
 Edmonton, AB, Canada
 Keqiang.hu@gmail.com

Abstract—In this paper, the transient heat conduction in a layered composite with an insulated interface crack parallel to the boundaries is investigated by using the dual phase lag (DPL) model. Fourier and Laplace transforms are applied and the mixed boundary value problem for the cracked structure under temperature impact is reduced to solving a singular integral equation. The temperature field in time domain is obtained and the intensity factor of temperature gradient is defined. Numerical studies show that overshoot phenomenon may occur due to the combined effect of the insulated crack and application of the DPL heat conduction model. The thermal conductivity and the phase lag parameters have strong influence on the dynamic intensity factor of temperature gradients. The results obtained by the dual phase lag model can be reduced to that by the hyperbolic model and that by the parabolic model.

Keywords- transient heat conduction; dual-phase lag model; non-Fourier heat conduction; Singular integral equation

I. INTRODUCTION

High-rate heat transfer has become a major concern in modern industries and accurate heat conduction analysis is of great importance for the material and structural integrity. For applications involving high power density, extremely short times or cryogenic temperatures, the classical parabolic heat diffusion theory as stipulated by Fourier's law of heat conduction becomes ineffective [1]. A unified heat conduction model that accounts for spatial and temporal effects in macro- and micro-scale heat transfer in a one temperature formulation has been proposed and was experimentally supported [2], namely the dual-phase-lag (DPL) model.

Inherent defects in materials such as dislocations and cracks may disturb the temperature distribution when thermal loading is applied to the material, and singularities may be developed in the neighborhood of discontinuities. Heat conduction problems of cracked materials using the classical Fourier heat conduction model have been investigated by some researchers [3, 4]. Some investigations on crack problems in thermo-elastic materials have been made using the hyperbolic heat conduction model. Transient temperature field

around a thermally insulated crack in a substrate bonded to a coating has been obtained by Chen and Hu [5] using the hyperbolic heat conduction model; and based on the same theory, Hu and Chen [6] obtained the transient temperature and thermal stress distributions around a partially insulated crack in a thermo-elastic strip. The problem of a finite crack in a material layer under the theory of non-Fourier heat conduction has been investigated by Wang and Han [7]. By applying the DPL model to a cracked half-plane under transient thermal loading, the dynamic temperature field around a partially insulated crack has been obtained [8].

To the author's knowledge, the transient interface crack problem in a layered composite under thermal loading by applying the dual phase lag model has not yet been reported in the literature. In this paper, we analyze the transient temperature field around an insulated interface crack in a layered composite under temperature impact using the dual phase lag model. The effect of the parameters of the dual phase lag model and the geometric size of the cracked body on the temperature disturbance field are investigated.

II. PROBLEM DESCRIPTION

Consider a thermo-elastic, double-layered structure containing an interface crack of length $2c$ parallel to the boundaries of the structure, as shown in Fig. 1. The thicknesses of the upper and lower layers are h_1 and h_2 , respectively. The layered structure is initially at the uniform temperature of zero, and is suddenly heated to a temperature, T_1 and T_2 on the upper and the lower boundaries, respectively, and $H(t)$ denotes the Heaviside step function. The crack surfaces are assumed to be thermally insulated, which indicates that the thermal transfer across the crack faces vanishes.

In order to account the effects of finite heat propagation and micro-structural interaction, the Fourier's law of heat conduction is modified to the DPL model [2],

$$q + \tau_q \frac{\partial q}{\partial t} + \frac{\tau_q^2}{2} \frac{\partial^2 q}{\partial t^2} = -k \cdot \left(\nabla T + \tau_T \frac{\partial}{\partial t} \nabla T \right). \quad (1)$$

where q is the heat flux, T is the temperature, k is the thermal conductivity of the material, ∇ is the spatial gradient operator, t is the physical time at which observation on heat transport is made, τ_q and τ_T are the phase lags of the heat flux and temperature gradient, respectively, which are two intrinsic thermal properties of the material. The heat flux precedes the temperature gradient for $\tau_q < \tau_T$, and the temperature gradient precedes the heat flux for $\tau_q > \tau_T$.

Conservation of the local energy with vanishing heat source applies [9]:

$$-\nabla q = \rho C_p \cdot \frac{\partial T}{\partial t} \quad (2)$$

where ρ and C_p are the mass density and the specific heat capacity, respectively.

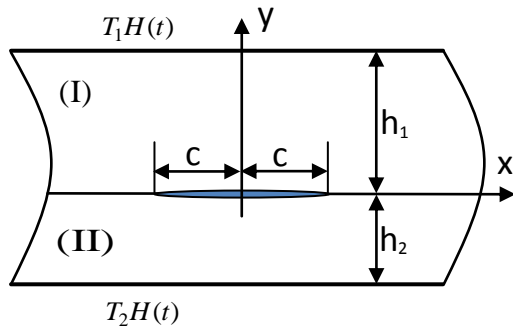


Figure 1. Geometry of cracked double-layered structure under transient thermal impact on the upper and lower surfaces

Incorporating (1) with (2) leads to the heat conduction equations in the following form

$$\nabla^2 T^{(1)} + R_1 \frac{\partial}{\partial t} (\nabla^2 T^{(1)}) = a^2 \left[\frac{\partial T^{(1)}}{\partial t} + \frac{\partial^2 T^{(1)}}{\partial t^2} + \frac{1}{2} \frac{\partial^3 T^{(1)}}{\partial t^3} \right]. \quad (3)$$

$$\nabla^2 T^{(2)} + R_2 \frac{\partial (\nabla^2 T^{(2)})}{\partial t} = \frac{a^2}{r_\alpha} \left[\frac{\partial T^{(2)}}{\partial t} + r_\tau \frac{\partial^2 T^{(2)}}{\partial t^2} + \frac{r_\tau^2}{2} \frac{\partial^3 T^{(2)}}{\partial t^3} \right]. \quad (4)$$

$$R_1 = \tau_T^{(I)} / \tau_q^{(I)}, \quad R_2 = \tau_T^{(II)} / \tau_q^{(I)} \quad (5)$$

$$r_\alpha = \alpha^{(II)} / \alpha^{(I)}, \quad r_\tau = \tau_q^{(II)} / \tau_q^{(I)}.$$

where $a = c/L$ is a characteristic length parameter of the material, the superscript “(1), (2)” represent the variables in the upper layer and the lower layer, respectively. It is noted that the following dimensionless variables have been used for simplicity:

$$T^{(1)} = T^{(I)} / T_1, \quad T^{(2)} = T^{(II)} / T_1, \quad L = \sqrt{\alpha^{(I)} \tau_q^{(I)}} \quad (6)$$

and the time have been normalized as $t / \tau_q^{(I)}$.

The heat conduction equations are subjected to the following boundary and initial conditions in the dimensionless form as

$$T^{(1)}(x, h_1, t) = 1, \quad (|x| < \infty, t > 0). \quad (7)$$

$$T^{(2)}(x, -h_2, t) = T_2 / T_1, \quad (|x| < \infty, t > 0). \quad (8)$$

$$q^{(1)}(x, 0^+, t) = q^{(2)}(x, 0^-, t), \quad (|x| \geq c). \quad (9)$$

$$T^{(1)}(x, 0^+, t) = T^{(2)}(x, 0^-, t), \quad (|x| \geq c). \quad (10)$$

$$\frac{\partial T^{(1)}(x, 0^+, t)}{\partial y} = \frac{\partial T^{(2)}(x, 0^-, t)}{\partial y} = 0, \quad (|x| < c). \quad (11)$$

$$T^{(j)} = 0, \quad \frac{\partial T^{(j)}}{\partial t} = 0, \quad \frac{\partial^2 T^{(j)}}{\partial t^2} = 0, \quad (t = 0, j = 1, 2). \quad (12)$$

III. METHOD OF THE PROBLEM

Application of Laplace transforms to (3, 4) leads to:

$$T^*(x, y, p) = \int_0^\infty T(x, y, t) \exp(-pt) dt \quad (13)$$

$$T(x, y, t) = \frac{1}{2\pi i} \int_{Br} T^*(x, y, p) \exp(pt) dp$$

where the superscript “*” denotes the quantities in the Laplace domain and Br stands for the Bromwich path of integration.

By considering the initial conditions and boundary conditions, we can obtain the appropriate temperature field in the Laplace domain by using Fourier transforms as

$$T^{*(1)}(x, y, p) = \int_{-\infty}^{\infty} \left[\begin{array}{l} D_1(\xi, p) \exp(my) \\ + D_2(\xi, p) \exp(-my) \end{array} \right] \exp(-ix\xi) d\xi, \quad (0 \leq y \leq h_1) \quad (14)$$

$$+ W_1(y, p)$$

$$T^{*(2)}(x, y, p) = \int_{-\infty}^{\infty} \left[\begin{array}{l} E_1(\xi, p) \exp(ny) \\ + E_2(\xi, p) \exp(-ny) \end{array} \right] \exp(-ix\xi) d\xi, \quad (-h_2 \leq y \leq 0) \quad (15)$$

$$+ W_2(y, p)$$

where $D_j(\xi, p)$, $E_j(\xi, p)$ ($j = 1, 2$) are unknowns to be determined and $m, n, W_1(y, p), W_2(y, p)$ are known functions.

Introduce the temperature density function as

$$\phi(x, p) = \frac{\partial T^{*(1)}(x, 0^+, p)}{\partial x} - \frac{\partial T^{*(2)}(x, 0^-, p)}{\partial x}. \quad (16)$$

It is clear from the boundary conditions (10) that

$$\int_{-c}^c \phi(t, p) dt = 0. \quad (17)$$

The satisfaction of the mixed boundary value problem on the crack face plane leads to the singular integral equation for $\phi(x, p)$ as follows

$$\int_{-c}^c \phi(t, p) \left[\frac{1}{t-x} + H(x, t, p) \right] dt = 2\pi u(b_2 - b_1). \quad (18)$$

where $H(x, t, p)$ is the kernel function and its expression is omitted here.

The solution of the singular integral equation (18) under the single-valuedness condition (17) may be expressed as [10]:

$$\phi(cx, p) = \Phi(x, p) / \sqrt{1-x^2}. \quad (19)$$

where $\Phi(x, p)$ is bounded and continuous on the interval $[-1, 1]$. From the properties of symmetry and the condition (17), it is seen that $\Phi(x, p)$ is an odd function of x , i.e., $\Phi(-x, p) = -\Phi(x, p)$.

By using the numerical method of Erdogan [10], Singular integral equations (17) and (18) can be solved at discrete points as

$$\sum_{k=1}^N \frac{1}{N} \Phi(t_k, p) \left[\frac{1}{t_k - x_r} + H(x_r, t_k, p) \right] = 2u(b_2 - b_1), \quad (r = 1, 2, \dots, N-1) \quad (20-1)$$

$$\sum_{k=1}^N \frac{\pi}{N} \Phi(t_k, p) = 0. \quad (20-2)$$

$$t_k = \cos[(2k-1)\pi/2N], \quad (k = 1, 2, \dots, N). \quad (20-3)$$

$$x_r = \cos(r\pi/N), \quad (r = 1, 2, \dots, N-1) \quad (20-4)$$

Once the function $\Phi(t, p)$ is obtained, the function $D_2(\xi, p)$ can be obtained by applying the Chebyshev quadrature for integration as

$$D_2(\xi, p) \equiv -\frac{1}{2\pi\xi G(\xi, p)} \sum_{m=1}^N w_m \Phi(x_m, p) \sin(x_m \xi) \quad (21-1)$$

$$x_m = \cos\left(\frac{2m-1}{2N}\pi\right), \quad (m = 1, 2, \dots, N) \quad (21-2)$$

$$w_m = \pi/N \quad (21-3)$$

The functions $D_1(\xi, p)$, $E_j(\xi, p)$ ($j = 1, 2$) can be expressed in terms of $D_2(\xi, p)$ as

$$\begin{aligned} D_1(\xi, p) &= -D_2(\xi, p) \exp(-2mh_1) \\ E_1(\xi, p) &= -\frac{mK_1(p)[1 + \exp(-2mh_1)]}{nK_2(p)[1 + \exp(-2nh_2)]} D_2(\xi, p). \\ E_2(\xi, p) &= \frac{mK_1(p)[1 + \exp(-2mh_1)]}{nK_2(p)[1 + \exp(2nh_2)]} D_2(\xi, p) \end{aligned} \quad (22)$$

IV. TEMPERATURE FIELD

The substitution of (21, 22) into (14, 15) can give the temperature in the Laplace domain, and the temperature in time domain can be obtained by applying the Laplace inverse transform.

Of particular interest are the temperature gradients in the cracked media under thermal loadings. A temperature gradient

is a physical quantity that describes in which direction and at how much rate the temperature changes the most rapidly around a particular location. The temperature gradients in the Laplace domain can be obtained as

The singular temperature gradients near the right crack tip in the Laplace domain can be obtained as

$$T_{,y}^{*(1)}(r, \theta, p) = -\frac{\Phi(1, p)\sqrt{c}}{2\sqrt{2}r} \cos\left(\frac{\theta}{2}\right). \quad (23-1)$$

$$T_{,y}^{*(2)}(r, \theta, p) = -\frac{K_1(p)}{K_2(p)} \frac{\Phi(1, p)\sqrt{c}}{2\sqrt{2}r} \cos\left(\frac{\theta}{2}\right). \quad (23-2)$$

$$T_{,x}^{*(1)}(r, \theta, p) = \frac{\Phi(1, p)\sqrt{c}}{2\sqrt{2}r} \sin\left(\frac{\theta}{2}\right). \quad (24-1)$$

$$T_{,x}^{*(2)}(r, \theta, p) = \frac{K_1(p)}{K_2(p)} \frac{\Phi(1, p)\sqrt{c}}{2\sqrt{2}r} \sin\left(\frac{\theta}{2}\right). \quad (24-2)$$

The temperature gradients near the crack tip in the radial direction in the Laplace domain can be obtained as

$$T_{,r}^{*(1)}(r, \theta, p) = -\frac{\Phi(1, p)\sqrt{c}}{2\sqrt{2}r} \sin\left(\frac{\theta}{2}\right). \quad (25-1)$$

$$T_{,r}^{*(2)}(r, \theta, p) = -\frac{K_1(p)}{K_2(p)} \frac{\Phi(1, p)\sqrt{c}}{2\sqrt{2}r} \sin\left(\frac{\theta}{2}\right). \quad (25-2)$$

where the subscript “ j ” ($j = x, y, r$) denote the temperature gradient in x , y and radial direction, respectively; (r, θ) are the polar coordinates measured from the crack tip defined by

$$r^2 = (x-c)^2 + y^2, \quad \tan(\theta) = y/(x-c). \quad (26)$$

In front of the crack tip at $\theta = -\pi$, the temperature gradient reaches the maximum value and the intensity factor of the temperature gradient (IFTG) near the crack tip can be defined as [11],

$$K_T^{*(1)}(p) = \lim_{r \rightarrow 0} 2\sqrt{r} T_{,r}^{*(1)}(r, \theta, p) \Big|_{\theta = -\pi} = \frac{\Phi(1, p)\sqrt{c}}{\sqrt{2}} \quad (27)$$

$$K_T^{*(2)}(p) = \lim_{r \rightarrow 0} 2\sqrt{r} T_{,r}^{*(2)}(r, \theta, p) \Big|_{\theta = -\pi} = \frac{K_1(p)}{K_2(p)} \frac{\Phi(1, p)\sqrt{c}}{\sqrt{2}} \quad (28)$$

and the radial intensity factor of the temperature gradient (RIFTG) near the crack tip can be defined as

$$K_r^{*(1)}(\theta, p) = \lim_{r \rightarrow 0} 2\sqrt{r} T_{,r}^{*(1)}(r, \theta, p) = -\frac{\Phi(1, p)\sqrt{c}}{\sqrt{2}} \sin\left(\frac{\theta}{2}\right). \quad (29)$$

$$K_r^{*(2)}(\theta, p) = \lim_{r \rightarrow 0} 2\sqrt{r} T_{,r}^{*(2)}(r, \theta, p) = -\frac{K_1(p)}{K_2(p)} \frac{\Phi(1, p)\sqrt{c}}{\sqrt{2}} \sin\left(\frac{\theta}{2}\right) \quad (30)$$

By applying the inverse Laplace transform, the near crack-tip temperature gradients in time domain can be obtained as

$$T_{,y}^{(1)}(r, \theta, t) = -\frac{K_T^{(1)}(t)}{2\sqrt{r}} \cos\left(\frac{\theta}{2}\right). \quad (31-1)$$

$$T_{,y}^{(2)}(r, \theta, t) = -\frac{K_T^{(2)}(t)}{2\sqrt{r}} \cos\left(\frac{\theta}{2}\right). \quad (31-2)$$

$$T_{,x}^{(1)}(r, \theta, t) = \frac{K_T^{(1)}(t)}{2\sqrt{r}} \sin\left(\frac{\theta}{2}\right). \quad (32-1)$$

$$T_{,x}^{(2)}(r, \theta, t) = \frac{K_T^{(2)}(t)}{2\sqrt{r}} \sin\left(\frac{\theta}{2}\right). \quad (32-2)$$

$$T_{,r}^{(1)}(r, \theta, t) = -\frac{K_T^{(1)}(t)}{2\sqrt{r}} \sin\left(\frac{\theta}{2}\right). \quad (33-1)$$

$$T_{,r}^{(2)}(r, \theta, t) = -\frac{K_T^{(2)}(t)}{2\sqrt{r}} \sin\left(\frac{\theta}{2}\right). \quad (33-2)$$

where the intensity factor of temperature gradient (IFTG) in the time domain, $K_T^{(j)}(t)$ ($j=1,2$) is given as

$$K_T^{(1)}(t) = \frac{\sqrt{c}}{2\sqrt{2\pi i}} \int_{Br} \Phi(1, p) \exp(pt) dp. \quad (34-1)$$

$$K_T^{(1)}(t) = \frac{\sqrt{c}}{2\sqrt{2\pi i}} \int_{Br} \frac{K_1(p)}{K_2(p)} \Phi(1, p) \exp(pt) dp. \quad (34-2)$$

and the radial intensity factor of temperature gradient (RIFTG) near the crack tip in time domain is

$$\begin{aligned} K_r^{(1)}(\theta, t) &= -\frac{\sqrt{c}}{2\sqrt{2\pi i}} \int_{Br} \Phi(1, p) \sin\left(\frac{\theta}{2}\right) \exp(pt) dp \\ &= -K_T^{(1)}(t) \sin\left(\frac{\theta}{2}\right) \end{aligned} \quad (35-1)$$

$$K_r^{(2)}(\theta, t) = -K_T^{(2)}(t) \sin\left(\frac{\theta}{2}\right). \quad (35-2)$$

It can be seen from (33) that the dynamic temperature gradients possess a $r^{-1/2}$ singularity near the crack tip, which is in agreement with the corresponding static thermal crack problem [3, 11]. The dynamic effect is merely introduced by the IFTGs, which are time-dependent as shown in (34, 35). It can be observed that the maximum temperature gradient appears at the angle $\theta = \mu\pi$, which corresponds to the lower and the upper crack surfaces near the crack tip; this conclusion is in agreement of the physical intuition that abrupt temperature changes occur near the crack tip. The effect of the geometric size h_1 and h_2 on the radial intensity factor of temperature gradient (RIFTG) is through the function $\Phi(1, p)$, and the geometric size does not affect the angular function of the temperature gradient.

V. NUMERICAL RESULTS AND DISCUSSION

The temperature field in the time domain can be obtained by applying the numerical inversion of Laplace transform, as detailed in Miller and Guy [12]. The geometric size of the composite is chosen as $h_1/c=1$, $h_2/c=2$, $L=1$, without loss of generality.

The temperature distribution in the cracked layers is shown in Figs. 2 and Figs. 3 for the cases of $k_1/k_2=0.5$ and

$k_1/k_2=2$, respectively. Other related material parameters of the two layers are assumed to be $\tau_q^{(1)} = \tau_q^{(2)} = 10^{-9} s$, $\tau_T^{(1)} = 2.0 \times 10^{-9} s$, $\tau_T^{(2)} = 0.5 \times 10^{-9} s$. The normalized temperature applied on the boundaries of the layers are assumed to be $T_1=1$, $T_2=2$.

For the case of $k_1/k_2=0.5$, the disturbance of the thermally insulated crack on the temperature field can be observed from the iso-temperature lines in Fig. 2, and there is a temperature jump across the crack faces. The interference of the insulated crack results in the higher temperature in the inner region of the heat conduction medium than that on the boundary, this is called temperature overshooting phenomenon, as shown in Fig. 2, which corresponds to the normalized time $t=2.0$. This temperature overshooting phenomenon is of great importance in thermal engineering applications such as safety design of the electronic or mechanical devices under severe thermal loadings [13]. Fig. 3 display the temperature distribution in the cracked layers for the case of $k_1/k_2=2$, temperature overshooting phenomenon is observed and there is a temperature gap across the crack. Comparing to Fig. 2, it can be seen that the temperature intensification around the crack varies as the thermal conductivity parameters changes.

Of much interest is the temperature distribution on the crack faces as the insulated crack interrupt the temperature in the cracked composite. The temperature on the crack faces and crack face extended lines is shown in Fig. 4 for different time points. It is observed that there is temperature jump across the insulated crack on the interface of the bonded layers, while outside the crack region the temperature on the interface is continuous. As the time changes, the temperature on crack faces and the extended lines changes accordingly. It can be seen that the temperature on part of the upper face may exceed the temperature on the boundary.

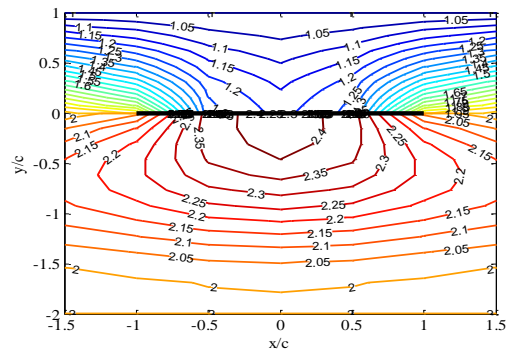


Figure 2. Temperature distribution in cracked layers when $k_1/k_2=0.5$ at $t=2.0$.

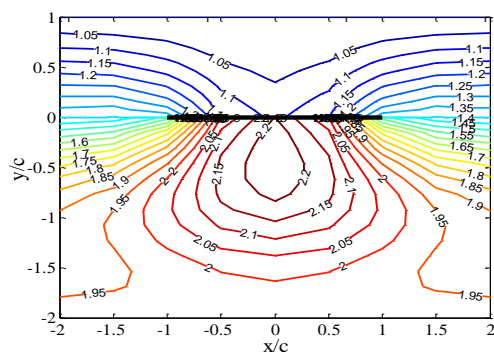


Figure 3. Temperature distribution in cracked layers when $k_1/k_2 = 2$ at $t = 2.0$.

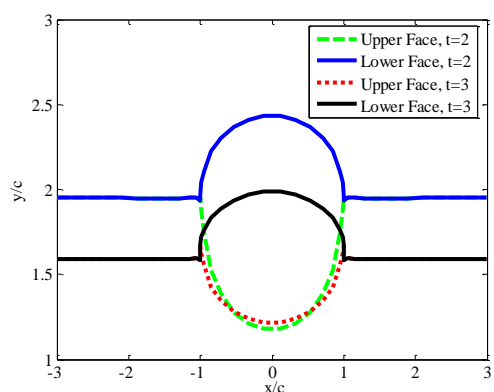


Figure 4. Temperature distribution on crack faces and extended lines when $k_1/k_2 = 0.5$.

VI. CONCLUSIONS

The transient temperature distribution in a layered composite with an interface crack under temperature impact loading has been studied using the dual phase lag model. The crack lies parallel to the boundary and is assumed to be thermally insulated. Fourier and Laplace transforms are applied to solve the temperature field, and the mixed boundary problem is reduced to solving a singular integral equation. An asymptotic analysis and inverse Laplace transform are applied to obtain the temperature field in the time domain and the intensity factor of temperature gradient is defined. Numerical studies show that overshoot phenomenon may occur due to the combined effect of the insulated crack and application of the DPL heat conduction model. The thermal conductivity and the phase lag parameters have strong influence on the dynamic intensity factor of temperature gradients.

VII. REFERENCES

- [1] D. S. Chandrasekharaiah, "Hyperbolic thermoelasticity: A review of recent literature," *Appl. Mech. Rev.*, vol. 51, pp. 705-729, 1998.

- [2] D. Y. Tzou, *Macro- to Micro-scale Heat Transfer: The Lagging Behavior*, Washington, DC: Taylor & Francis, 1997.
- [3] G. C. Sih, "Heat conduction in the infinite medium with lines of discontinuities," *ASME J. Heat Transfer*, vol. 87, pp. 283-298, 1965.
- [4] C. Y. Chang and C. C. Ma, "Transient thermal conduction of a rectangular plate with multiple insulated cracks by the alternating method," *Int. J. Heat Mass Transfer*, vol. 44, pp. 2423-2437, 2001.
- [5] Z. T. Chen and K. Q. Hu, "Hyperbolic heat conduction in a cracked thermoelastic half-plane bonded to a coating," *Int. J. Thermophys.*, vol. 33, pp. 895-912, 2012.
- [6] K. Q. Hu and Z. T. Chen, "Thermoelastic analysis of a partially insulated crack in a strip under thermal impact loading using the hyperbolic heat conduction theory," *Int. J. Eng. Sci.*, vol. 51, pp. 144-160, 2012.
- [7] B.L. Wang and J. C. Han, "Fracture mechanics associated with non-classical heat conduction in thermoelastic media," *Sci. China, Phys. Mech. & Astron.*, vol. 55, pp. 493-504, 2012.
- [8] K. Q. Hu and Z. T. Chen, "Transient heat conduction analysis of a cracked half-plane using dual-phase-lag theory," *Int. J. Heat Mass Transfer*, vol. 62, pp. 445-451, 2013.
- [9] H.S. Carslaw and J.C. Jaeger, *Conduction of heat in solids*, Oxford: Oxford Science Publications, Clarendon Press, 1990.
- [10] F. Erdogan, "Complex function technique" in A. C. Eringen (Editor), *Continuum Physics*. Vol. 2, pp. 523-603, New York: Academic Press, 1975.
- [11] D. Y. Tzou, "The singular behavior of the temperature gradient in the vicinity of a macrocrack tip," *Int. J. Heat Mass Transfer*, vol. 33, pp. 2625-2630, 1990.
- [12] M.K. Miller and W.T. Guy, "Numerical inversion of the Laplace transform by use of Jacobi polynomials," *SIAM J. Numer. Anal.*, vol. 3, pp. 624-635, 1966.
- [13] M. Xu, J. Guo, L. Wang, and L. Cheng, "Thermal wave interference as the origin of the overshooting phenomenon in dual-phase-lagging heat conduction," *Int. J. Thermal Sci.*, vol. 50, pp. 825-830, 2011.